Dissertation Prospectus

The Effects of Aerosol on the Dissipation of Arctic Mixed-Phase Clouds

Lucas Sterzinger

Atmospheric Science Graduate Group

University of California, Davis

Committee Members

Ian Faloona, Chair

Adele L. Igel

Joseph Sedlar

Shu-Hua Chen

Paul Ullrich

August 15, 2020

Contents

1 Introduction

The Arctic has been shown to be extremely sensitive to a warming climate, with data showing the Arctic warming anywhere from 1.5 - 4.5x the global mean warming rate (Holland and Bitz, 2003). Clouds, in general, directly affect the surface energy budget and can act as net-warming or net-cooling influences, depending on their specific physical characteristics. Of particular note in the Arctic environment are low-level, boundary layer stratocumulus clouds which cover large fractions of the Arctic throughout the year (Shupe, 2011). They have been found to be a net-warming influence on the surface, except for a short period in the summer when they act as a net-cooling influence (Intrieri et al., 2002; Shupe and Intrieri, 2004). These clouds tend to be mixed-phase, meaning they simultaneously contain liquid and ice water. Shupe et al. (2006) found that mixed-phase clouds accounted for 59% of the clouds identified during a year-long campaign on an icepack in the Beaufort Sea. Mixed-phase clouds are a known problem for numerical models of all scales (Morrison et al., 2012, 2011; Klein et al., 2009); understanding the processes involved in the formation and dissipation of these clouds is essential to understanding the energy balance in the Arctic and for proper representation in models.

These Arctic mixed-phase boundary layer clouds often last for days at a time, and dissipate in a matter of hours (Shupe, 2011; Morrison et al., 2012). This persistence is surprising given the inherit microphysical instability of mixed-phase clouds, which are affected by the Wegener-Bergeron-Findeisen (WBF) process (Wegener, 1911; Bergeron, 1935; Findeisen, 1938) in which ice grows via deposition at the expense of liquid water. Without processes maintaining supercooled liquid water, the WBF process would work to glaciate (i.e. completely convert to ice) the cloud. The mechanisms behind this persistence and rapid dissipation are not well known (Morrison et al., 2012). It has been hypothesized that the low cloud condensation nuclei (CCN, a subset of aerosol, which are required for cloud droplet formation) concentrations in the Arctic could have an effect on cloud dissipation. Mauritsen et al. (2011) coined the term "tenuous cloud regime" to describe the regime where clouds are limited by CCN availability, and showed that Arctic CCN concentrations are often low enough to affect cloud formation. Modeling studies (Birch et al., 2012; Stevens et al., 2018; Sotiropoulou et al., 2019) have supported the existence of the tenuous cloud regime, but none of these studies has focused directly on the role of limited CCN on the dissipation of Arctic mixed-phase boundary layer clouds. The goal of the proposed research is to investigate the dissipation response to limited CCN. Specifically, the following questions will be addressed:

Q-1 How sensitive are Arctic mixed-phase boundary layer cloud to a decrease in CCN, both above and below cloud?

Q-2 What is the dependence of dissipation caused by low CCN to ice nuclei (IN)? What role does the WBF process play?

Q-3 How does the structure of the boundary layer affect CCN-limited dissipation?

Section 2 will review the applicable literature and assess the current state of knowledge, Section 3 will discuss details on the observations and modeling methods to be used, Section

4 will provide an overview of the specific tasks needed to answer the questions above, and Section 5 will discuss some of the preliminary results currently available.

2 Present State of Knowledge

Morrison et al. (2012) presented an overview of the long-term persistence of mixed-phase Arctic clouds. These clouds are maintained by cloud-scale updrafts which, if strong enough, can create situations where the atmosphere is supersaturated with respect to both ice and liquid, meaning both supercooled liquid water droplets and ice crystals will grow from available water vapor, thus negating the WBF process (Korolev, 2007). High supercooled liquid water droplet concentrations near cloud top promote radiative cooling, which creates a buoyant overturning circulation and further enhances the cloud (Brooks et al., 2017). Moisture inversions co-located with temperature inversions at boundary layer top are not uncommon in the Arctic boundary layer, occurring upwards of 90% of the time in the winter and 70-80% in the summer (Naakka et al., 2018; Egerer et al., 2020). Sedlar et al. (2011) found that moisture inversions occurred 75 - 80% of the time specifically with low Arctic clouds. Cloud-top entrainment can thus act as a source of water vapor (Solomon et al., 2011; Sedlar et al., 2012; Sedlar and Tjernström, 2009). These processes allow the cloud to persist despite the low heat and moisture fluxes at the surface and, if the cloud is decoupled from the surface, moisture entrainment may be the only source of vapor (Sedlar et al., 2012). The presence (or lack) of a moisture inversion will be one of the subjects of study for Q-3.

In contrast to low-level clouds at lower latitudes, Arctic boundary layer clouds tend to warm the surface. Since these clouds are located near the high-albedo ice-covered surface, absorbed shortwave radiation is minimally impacted by the presence of clouds and the surface temperature is primarily forced by longwave radiation emitted by the cloud. In the summer where more of the Arctic surface is comprised of open water and melt ponds, surface albedo is lower and these clouds instead act to cool the atmosphere (Intrieri et al., 2002; Tjernström et al., 2014).

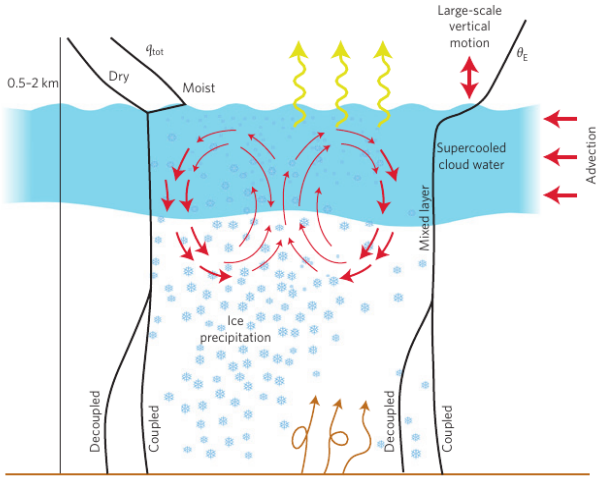

Figure 1: Overview of processes that affect Arctic mixed-phase boundary layer clouds. Figure taken from Morrison et al. (2012)

A cartoon illustration of the processes that dominate Arctic mixed-phase boundary layer clouds is shown in Figure 1, which was taken from Morrison et al. (2012). The cloud depicted is a typical Arctic boundary layer mixed-phase cloud: a layer of supercooled liquid water exists at cloud top with ice precipitating below. The cartoon shows example temperature and moisture profiles for coupled and decoupled cases. In the decoupled case,

small moisture and temperature inversions between the cloud layer and the surface prevent turbulent interactions between the surface mixed-layer (SML) and cloud mixed-layer (CML). Investigating the impact of coupled versus decoupled SMLs on dissipation will be examined as part of Q-3. It should be noted that the SML is not the same as the surface layer described in Monin–Obukhov similarity theory. Instead, it refers to a portion of the boundary layer mixed primarily by surface turbulent fluxes. The CML, in contrast, is mixed primarily by buoyant circulation driven by cloud-top radiative cooling (Brooks et al., 2017).

CCN availability has a direct affect on cloud properties; an increase in CCN concentration will divide the available water vapor between more activated CCN, resulting in more cloud droplets of smaller diameters. The resulting cloud is more reflective to shortwave radiation, a phenomenon known as the Twomey effect (Twomey, 1977). While this causes surface cooling due to reflectance of incoming shortwave radiation back into space, in the Arctic the Twomey Effect has a competing surface warming due to increase cloud longwave emissivity (Garrett et al., 2002; Garrett and Zhao, 2006).

Little has been done until recently to examine the effect of abnormally low CCN in the Arctic. Mauritsen et al. (2011) proposed, through observation, the existence of a tenuous cloud regime, where the cloud structure was limited by CCN concentration (which in lower-latitudes ranges from 100 - 1000 cm^{-3} or more, but can be as low as 1 cm^{-3} in the Arctic). Birch et al. (2012) found that their model, which prescribed CCN at 100 cm^{-3}, did not adequately model a decrease in cloud cover observed during the ASCOS field campaign until the CCN concentration was reduced to either 1 or 2 cm^{-3}. In her masters degree thesis, Tong (2019) examined modeled cloud dissipation in response to various CCN and ice nuclei (IN) concentrations. In the study, the cloud dissipated even when CCN concentrations were fixed in time, which prevented strong conclusions on the role of CCN concentrations as a *cause* of dissipation from being made. That being said, different CCN treatment did result in variations in the dissipation timescale, indicating that the dissipation of the cloud was, at minimum, sensitive to CCN concentrations. Cloud dissipation was found to be more sensitive to CCN decreases in the boundary layer than in the free troposphere. Mixing within the boundary layer is strong and allows for exchange of CCN between the sub-cloud and cloud layers, whereas this CCN transport is much weaker between the cloud layer and the free troposphere.

However, with few local boundary layer aerosol sources outside of the summer months (where open water is more common), long-range tropospheric transport from lower latitudes is, potentially, a large source of aerosol in the Arctic (Kupiszewski et al., 2013; Cheng et al., 1993; Rahn et al., 1977) with entrainment by cloud-top mixing acting as a source of aerosol in the boundary layer (Igel et al., 2017; Shupe, 2011). Igel et al. (2017) found that a source of boundary layer aerosol was direct entrainment of tropospheric aerosol directly into the boundary layer. Additionally, cloud-mediated transport accounted for 35% of the increase in boundary layer aerosol. This cloud-mediated transport occurs when clouds extend above the capping inversion of the boundary layer (often by 100 - 200 m), which happens more frequently than not in the Arctic (Sedlar and Tjernström, 2009; Sedlar et al., 2012). In this scenario, cloud droplets may nucleate directly onto non-entrained tropospheric CCN, some of which may be regenerated in the boundary layer. However, the authors note that very few tropospheric aerosol were present near the surface, indicating that surface-based

measurements would be unable to determine the presence (or lack thereof) of tropospheric aerosol in the ABL. Investigation of the relative impacts of tropospheric versus boundary layer CCN will be a key focus of Q-1.

3 Methods

Properly answering the questions posed in Section 1 will require analysis of both observational data and model results. The United States Department of Energy (DOE) Atmospheric Radiation Measurement (ARM) user facility has a permanent field observatory at Utqiaġvik (formerly known as Barrow), Alaska, as well as a mobile facility currently on an extended deployment to Oliktok Point, Alaska. These sites, as well as field campaigns performed on ships within the Arctic ice sheet, will serve as observational datasets from which cases will be selected. Cases will be selected based on observed cloud dissipation and measured aerosol concentrations. Cloud dissipation can be recognized by radar, lidar, and radiometer data, and CCN concentration can be measured directly by surface and balloon-borne CCN counters.

Observed values will be used to create model simulations for each case. The Colorado State University Regional Atmospheric Modeling System (RAMS; Cotton et al. 2003) will be used to run large-eddy resolving simulations (LES) of the Arctic boundary layer, initialized from data from a case selected for study. The RAMS model has been shown to perform well at LES scales (e.g. Cotton et al. 1992; Jiang et al. 2001; Jiang and Feingold 2006). RAMS includes cloud and ice nucleation schemes outlined in Saleeby and Cotton (2004) and DeMott et al. (2010), respectively. Radiation parameterization is provided by the Harrington scheme (Harrington, 1997), and turbulence is parameterized by the Deardorff level 2.5 scheme, which parameterizes eddy viscosity as a function of turbulent kinetic energy (TKE).

RAMS uses a double-moment bulk microphysics scheme (Walko et al., 1995; Meyers et al., 1997; Saleeby and Cotton, 2004) that predicts the mass and number concentration of eight hydrometeor categories: cloud droplets, drizzle, rain, pristine ice, aggregates, snow, hail, and graupel. Each of these hydrometeor categories is represented by a generalized gamma distribution which is characterized by a shape parameter (supplied by the user at model runtime) and a characteristic diameter. The scheme simulates nucleation (cloud and ice), vapor deposition, evaporation, collision-coalescence, melting, freezing, secondary ice production, and sedimentation. Cloud droplets and drizzle may be nucleated directly from water vapor, with nucleated droplets with diameters < 40 μm classified as cloud and droplets with diameters between 40 and 80 μm classified as drizzle. The size partitioning is to improve representation of larger droplets, which are much more likely to collide and coalesce (Saleeby and Cotton, 2004). Ice crystals are heterogeneously nucleated based on the formula by DeMott et al. (2010), and will be discussed further in Section 4.3.

The aerosol treatment, outlined in Saleeby and van den Heever (2013), includes both wet and dry deposition, as well as depletion by cloud nucleation and regeneration by evaporation. Regenerated aerosol are placed in a separate 3D variable, allowing for more detailed analysis on aerosol regeneration. Aerosol concentration in RAMS is represented by a log-

normal distribution where the initial distribution median radius is supplied by the user at model runtime and the distribution standard deviation is fixed within the model source code. During RAMS' development, a series of Lagrangian parcel bin models (based on Köhler theory) were run to simulate aerosol activation and droplet nucleation for various distributions and conditions (Saleeby and van den Heever, 2013). These results were compiled into a 5-dimensional lookup table of activation fractions which are hard-coded into RAMS and depend on vertical velocity, temperature, number concentration, median radius, and soluble fraction ε.

When cloud nucleation occurs, the aerosol distribution is divided into 100 bins over an optimized size range (which varies based on median radius). The fraction of aerosol to activate is calculated based on the lookup tables described above. Aerosol mass and number are then removed by subtracting the number of newly formed cloud droplets from the large end of the binned aerosol distribution. A new median radius is computed and used to redistribute the remaining number concentration and mass according to the lognormal distribution. This binned method ensures that removing a set number from the distribution does so preferentially to larger aerosol. The aerosol mass that was removed during nucleation is stored as a 3D variable containing the total aerosol mass contained within the cloud droplets. This mass is conserved and transferred through hydrometeor processes, and is used to regenerate aerosol in the event of hydrometeor evaporation (or sublimation, in the case of ice).

The observations will be used to generate an initial sounding and CCN concentration for RAMS, which in turn will simulate the dissipation event. A horizontal domain of 6x6 km with a spacing of 62.5 meters, and a vertical domain of 200 levels with spacing of 6.25 meters will be used. The lateral edges of the model will have cyclic boundary conditions, allowing features that pass through one side of the domain to emerge from the other. While soundings (both observed and interpolated between launches) are available at both measurement sites, they do not contain information on the liquid water/ice content of the cloud. To properly initialize RAMS, liquid water will have to be manually added to sounding data. In the absence of observed vertical profiles of liquid water content, a linear profile of water mass (zero at cloud base and maximum at cloud top) will be added, with a slope chosen such that integrating the liquid profile from cloud base to cloud top yields the observed liquid water path.

4 Research Tasks

4.1 Identification of Tenuous Cloud Dissipation Cases

A limitation of the previous work done by Tong (2019) was the focus on a single case. In this proposed work, I will attempt to identify a wide range of cases (ideally around 3-7) that represent a variety of atmospheric conditions. Specifically to address Q-3, I aim to represent a range of boundary layer conditions, such as cases where cloud tops are either below or above the temperature inversion, the presence or lack of a moisture inversion, as well as coupled and decoupled surface layers. Before modeling can be done, potential cases must

be identified. Specifically, data from the DOE ARM sites along the north slope of Alaska will be used to identify periods of decreased cloudiness and CCN concentration. Along with the permanent site at Utqiaġvik, the long-term mobile facility at Oliktok Point will be used to identify cases. In addition, data from ship-based field campaigns such as ASCOS (Tjernström et al., 2014) may be used, though preference will be given to the ARM facilities.

Data from these sources will be analyzed to find periods of cloud dissipation coincident with a decrease in surface aerosol concentration. Both sites contain, at minimum, continuous measurements from a Ka-band ARM Zenith Radar (KAZR), a microwave radiometer (MWR), and a surface-based condensation particle counter (CPC). KAZR radar provides reflectivity and cloud base/height estimates. The MWR data is used by the MWRRETV2 Value Added Product (VAP) which uses methods outlined in Turner et al. (2007) to estimate liquid (LWP) and ice water path (IWP) as well as estimates of cloud top/base height. The CPC instrument provides number concentration for aerosols between the sizes of 30 - 3000 nm.

To identify potential cases, the CPC data will be analyzed in Python to find periods within a 4-hour moving window where number concentrations dropped from values > 50 cm^{-3} to < 20 cm^{-3}. The window is moved forward in time in 15-minute increments. This process creates a database of possible cases which can then be processed further. Radar data is acquired for the times listed in the domains, and a visual inspection of CPC data plotted alongside KAZR reflectivity plots is used to determine whether the cloud is dissipating coincident to a drop in aerosol concentration.

The Oliktok Point station is located near oil fields in Pruhoe Bay, AK. Gunsch et al. (2019) found that the OLI site was constantly influenced by emissions from the oil field, which increased the measured CCN concentrations and decreased the mean effective radii of measured cloud droplet distributions. These emissions are also able to travel to the site at Utqiaġvik, contaminating both available sites. Since these emissions were found to be primarily trace gases and ultrafine particles (< 50 nm), the fine-CPC ($30 - 3000$ nm) was used in lieu of the ultrafine CPC ($3 - 3000$ nm) to filter out some of the influence of the emissions.

4.2 Modeling the Effects of Aerosol on Cloud Dissipation

A suite of experiments will be performed to address the questions posed in Section 1. Properly answering Q-1 requires modifications to RAMS' aerosol/CCN treatment. RAMS has the ability to simulate CCN depletion via nucleation and deposition, and regenerate them upon hydrometeor evaporation. This treatment will be used, with some modification, to ensure that the simulation is as physically realistic as possible, and to attempt to validate the results of Igel et al. (2017) in which regenerated tropospheric CCN act as a CCN source within the boundary layer.

In the prior work done on this project in Tong (2019), the control case (which had no aerosol sources/sinks) dissipated without any change to CCN treatment. In the proposed work, a stable control simulation will be required for each case, against which simulated dissipations can be compared. Having a stable control simulation will allow proper investi-

Experiment Name	Bottom Layer	Free Troposphere
CON	Reset	Reset
SFC	Decay	Reset
FT	Reset	Decay
SFC-FT	Decay	Decay

Table 1: Overview of proposed experiments. Aerosol concentrations will either be reset back to initial values, or decayed based on observed timescale. In the boundary layer, only the bottommost layer of the atmosphere will be reset/decay for CON-SFC and all experiments.

gation of the microphysical processes that lead to dissipation in the tenuous cloud regime and uncover aerosol/boundary layer processes critical to the dissipation of these clouds. The stability of the control simulation will allow for investigation of "trigger" events, such as critical CCN or IN concentrations, that would not be identifiable in the setup of Tong (2019).

To properly investigate the processes behind the dissipation of tenuous regime clouds, a suite of experiments will be performed to fully understand the microphysics involved. First and foremost, a proper control simulation is required. The proposed control, unlike Tong (2019), will utilize RAMS' aerosol depletion and regeneration treatment to provide a more physical representation of the in-cloud processes. To provide a suitable control, CCN concentrations will be held constant in both the boundary layer and free troposphere. In Tong (2019) the boundary layer CCN concentration was held constant from the surface to cloud base. However, CCN were being reset too close to the cloud, and the constant reset was acting as an infinite source of CCN mixed directly into the cloud, causing nonphysical runaway cloud droplet nucleation. To mitigate this, only the lowest model level will be reset instead of the entire boundary layer both to simulate a surface source of aerosol and to allow for enough distance between cloud base and the CCN-reset level.

Table 1 lists the proposed experiments. CON represents the control simulation discussed above, in which both the bottommost layer and the free troposphere CCN concentrations will be held constant. The remaining three experiments represent 1) forcing the surface CCN concentration to decay while keeping the FT constant, 2) forcing the FT CCN to decay while keeping the surface constant, and 3) forcing both the surface and the FT to decay, eventually removing all CCN sources from the simulation. To properly address all proposed research questions, 5-minute output from RAMS will be analyzed (primarily using Python) to investigate the processes involved and their divergence from the stable CON simulation. Specifically, profiles and timeseries of parameters such as CCN and cloud masses/number concentrations, liquid and ice hydrometeor masses and number concentrations, thermodynamic structure, and buoyant, turbulent, and radiative surface fluxes will be examined. These parameters capture a large portion of the processes involved, and understanding the interaction between them will be key to answering all questions listed in Section 1.

As both the DOE measurement sites (Utqiaġvik and Oliktok Point) are on the coast, prevalent wind directions will be used to determine surface type in the model. If the winds are primarily from the north, the surface will be specified as ice; otherwise, the surface will be specified as land. This will primarily effect the surface radiative and specific heat fluxes.

Over the ocean ice, high albedo reflects a large amount of incoming shortwave radiation, and the ice pack maximum temperature is locked at the melting point of ice. Conversely, over the land, darker vegetation and soil means more absorbed shortwave radiation, as well as stronger specific heat fluxes. If possible, cases advected from both directions will be analyzed and compared.

4.3 Modeling of Ice Nuclei

A key part of the dissipation of Arctic mixed-phase boundary layer clouds is the WBF process. This process occurs in mixed-phase clouds in temperatures ranging from -40 to 0 degrees celsius, where supercooled liquid droplets coexist with ice crystals. In these temperatures, there exists a range of water vapor pressures in which an environment may find itself supersaturated with respect to ice, but subsaturated with respect to water. Under these conditions, the liquid water will evaporate and act as a source of water vapor. The ice, conversely, finds itself in a supersaturated environment and thus deposition of water vapor onto the ice is needed to bring the environment into equilibrium, which acts as a sink of water vapor. The combined effect of these processes is that the ice crystals will grow at the expense of the liquid water. In order for a mixed-phase cloud to persist in the fashion observed in Arctic mixed-phase boundary layer clouds, processes must counteract this microphysical instability. If updrafts are strong enough, the atmosphere can be supersaturated with respect to both ice and water, promoting the growth of liquid water droplets (Korolev, 2007)

Studies (e.g. Prenni et al. 2007; Morrison et al. 2011) show an increase of ice nuclei leads to rapid transformation of mixed-phase clouds into all-ice clouds. Ice nuclei (IN), which exist as a subset of aerosol, are poorly understood and occur much less frequently in our atmosphere. While CCN concentrations generally range from between 10-1000 cm^{-3} or more, IN concentrations are often 10^{-5} - 0.1 cm^{-3} (DeMott et al., 2010). To examine the effect of IN on the cloud dissipation and properly address Q-2, the suite of experiments described in Section 4.2 will be simulated with various IN concentrations. IN concentrations in RAMS are parameterized by DeMott et al. (2010), in which the diagnosed N_{IN} is a function of both number concentration of aerosol ($n_{aer,0.5}$; number of aerosol >0.5 μm in diameter) and air temperature. RAMS has the option to calculate $n_{aer,0.5}$ on-the-fly, or hold it at a constant value. Tong (2019) chose the latter option, and showed best results with $n_{aer,0.5}$ set to 5 mg^{-1} which will be used as a starting point in this study. Various values of $n_{aer,0.5}$ will be tested with the intention of observing changes in the WBF process and its response to CCN-limited dissipation.

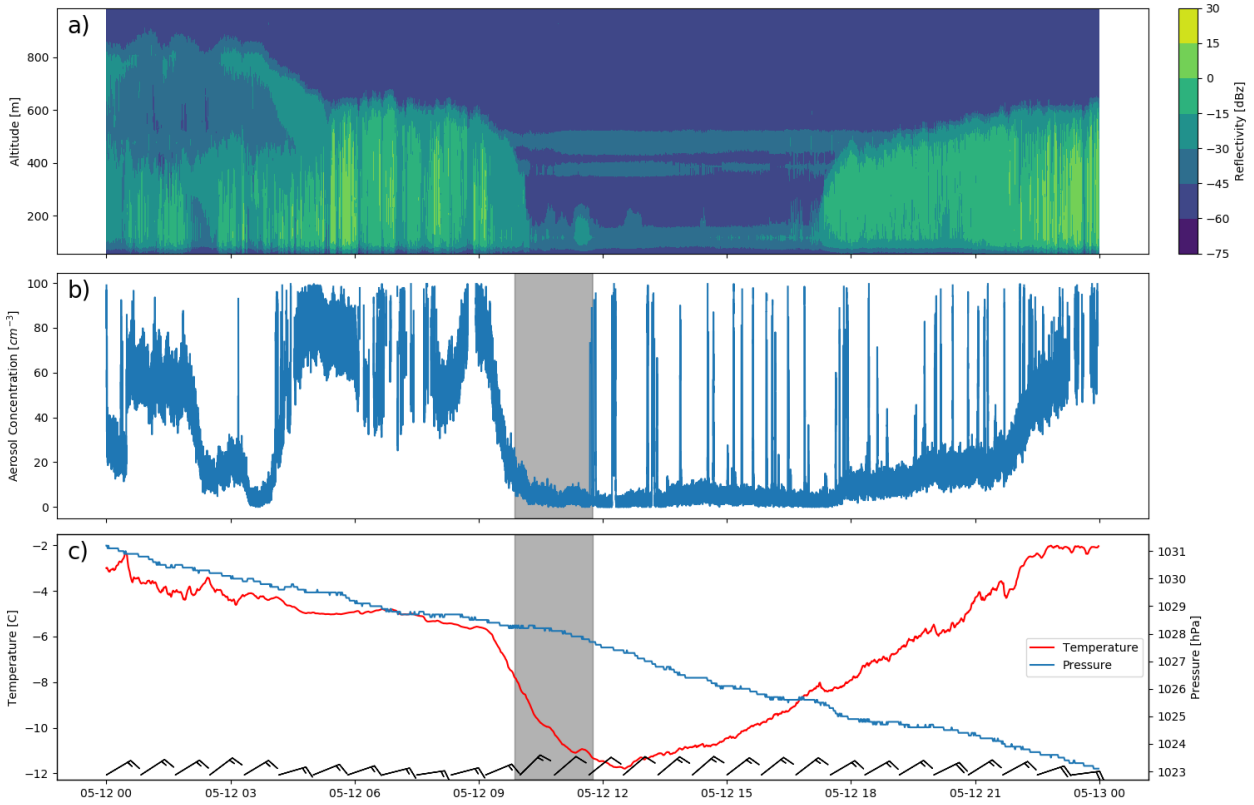

Figure 2: Timeseries of ground-based measurements at Oliktok Point for May 12, 2017. a) Ka-Band ARM Zenith Radar reflectivity b) CPC fine aerosol particle concentration c) Temperature, pressure, and wind barbs. The shaded region represents nighttime.

5 Preliminary Results

5.1 Case Identification

Through the process discussed in section 4.1, a single case has been identified to date. Figure 2 represents a suite of measurements taken at the Oliktok Point, AK ARM facility (OLI). At 0900 UTC on May 12, 2017 (1:00 AM local time), a cloud observed by the KAZR dissipated coincidentally with a decrease in aerosol measured at the surface with the CPC. In the hours before dissipation, aerosol concentrations remained relatively steady at $\sim$ 80 cm^{-3}. At 0900 UTC, both the cloud reflectivity and aerosol concentration decrease significantly. The cloud dissipates, and the aerosol concentration flattens out to $\sim$ 3 cm^{-3}. After approximately 7 hours of cloud-free conditions, a new cloud layer begins to develop as aerosol increases. Winds were primarily out of the northeast, meaning the clouds were being advected from over the ocean. Satellite imagery indicates that during this period, the ocean north of the Oliktok Point station was still covered in ice.

At time of dissipation surface temperatures dropped drastically, from -6°C to -12°C in the span of two hours. The dissipation occurred at 1:00 am local time, during the short period in which the sun has set in the Arctic spring (night time is shaded in grey). As such, incoming shortwave radiation was at a minimum and longwave radiation from the low

cloud layer was acting to warm the surface. As the cloud dissipated, this forcing left with it, causing a sharp decrease in temperature. Shortly after sunrise, surface temperatures begin to rise steadily. As the cloud re-forms and thickens, the temperature flattens out slightly above the initial temperature before dissipation.

The pressure during the 24 hours plotted in Figure 2 decreases linearly from 1031 hPa at 0000 UTC on May 12th to 1023 hPa at 0000 UTC on May 13th. Analysis of synoptic-scale patterns shows a high-pressure system located over the Beaufort Sea north of the OLI site move out of the area. It proves difficult to distinguish between a microphysically-forced dissipation (like the tenuous cloud regime that is the focus of the proposed research) and dynamically-forced dissipation. While no significant changes in the synoptic-scale flow occurred during the period of cloud dissipation, winds did shift to be more northward during the clear-sky period. MODIS data from Aqua and Terra satellites were analyzed (not shown). A large cloud deck is observed to dissipate between satellite passes and slowly reform, eventually covering the OLI site. It is this author's conclusion that while some large-scale airmass advection may have been present, the observed dissipation was mainly driven by local factors and qualifies for study.

5.2 Modeling

Data from the case discussed above were used to initialize RAMS. As discussed in Section 3, liquid water needed to be added to the sounding. The first available pre-dissipation balloon launch was at 2329 UTC on May 11th, 9 hours before the cloud dissipation event. The observed LWP at the time of balloon launch was 45 g m^{-2} within a 300 m thick cloud layer, and the liquid water profile added to the sounding has a maximum at cloud top of 0.215 g kg^{-1}.

To minimize wait time for model completion during case setup, the completed simulations have been run on a limited domain of 32x32 grid points (4 km^2) instead of the 96x96 grid points (36 km^2) of the anticipated final simulations. The vertical grid is the same in both scenarios: 200 levels spaced 6.25 m apart, for a domain height of 1.25 km. This horizontal domain shrinking was done to decrease the model runtime for a 24-hour simulation from over two full days to a few hours. We don't anticipate increasing the domain size to have a drastic impact, preliminary tests show it improves numerical issues with the small domain tests, explained further below.

RAMS was run for the first hour without the ability to form liquid hydrometeors other than cloud droplets. This spin-up time serves to promote the development of smaller-scale circulations and turbulence that, in the absence of strong surface fluxes, are needed to sustain the cloud and prevent the model from "raining out". Attempts to simulate this case without the spin-up time resulted in premature dissipation and an unstable cloud, even without decreasing CCN availability.

The control (CON) simulation for the May 12, 2017 case described in Section 5.1 is shown in Figure 3 with horizontally-averaged time series of a) cloud water mass, b) CCN concentration, c) rain water mass and d) ice water mass. In this simulation, non-cloud liquid hydrometeors were suppressed for the first hour as described above, and can be seen by the

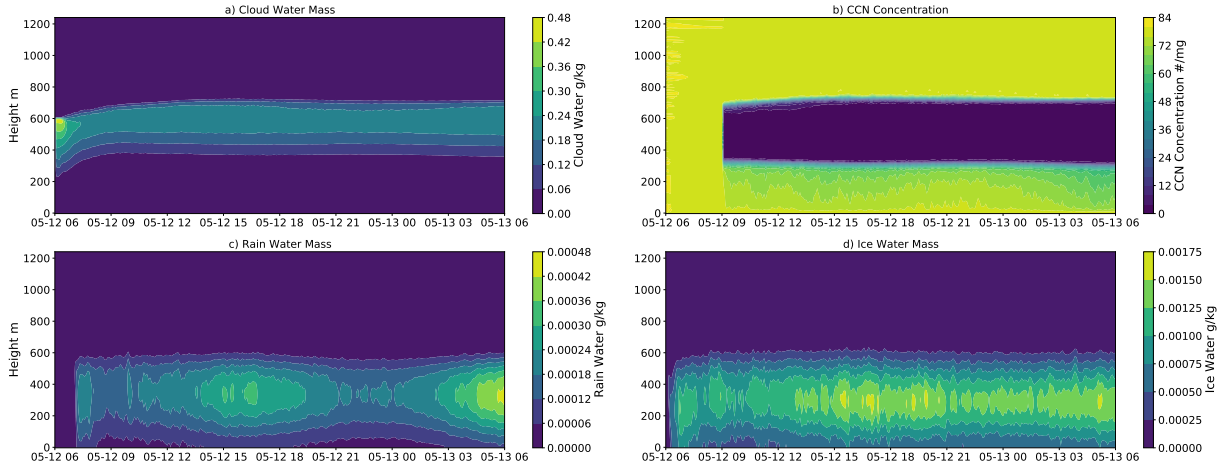

Figure 3: Control simulation for the May 12, 2017 case. a) Cloud water mass (g/kg) b) CCN Concentration (#/mg) c) Rain water mass (g/kg) and d) Ice Water Mass (g/kg)

lack of rain water in Figure 3c. CCN concentrations were kept constant for the first three hours, with no sources or sinks. After the third hour (0900 UTC), CCN were allowed to be depleted by the cloud and regenerated below. CCN levels are continually reset to the initial value of 80 mg^{-1} both above cloud top and in the very lowest level of the boundary layer. This is apparent by the immediate drop in CCN concentrations within the cloud at 0900 UTC in Figure 3b, with the tropospheric concentration constant above the cloud and slight decreases under the cloud. A small band of constant CCN is visible at the very bottom of the atmosphere where CCN are being reset in the bottommost model level.

Worth noting here are the small-scale fluctuations in rain and ice mass observed in 3c and 3, and point towards possible numerical instability in the model. The simulation shown in Figure 3 is being simulated on the limited 32x32 (2 km^2) domain explained above, and the small horizontal extent of the model domain is likely responsible for the observed instability.

Despite its internal fluctuation, the cloud itself is quite stable, which is a criteria needed in order to have a satisfactory control simulation against which to make comparisons. The cloud is able to maintain itself consistently for the 24 simulated hours, with temporally-consistent cloud top/base heights and ice precipitation amounts. The ice mass is, in general, an order of magnitude greater than the rain water mass. This aligns well with the structure of these clouds outlined in Section 2 and shown in Figure 1 in which a layer of supercooled liquid water cloud droplets form ice precipitation, creating a profile in which the liquid layer is situated above the ice layer.

6 Timeline

It is my goal to have cases selected and transition to full-time analysis by the end of 2020. While the experimental simulations outlined in Section 4.2 will provide a large amount of data to analyze, the research questions outlined in this document may require additional simulations as additional questions or uncertainties evolve over the course of the project.

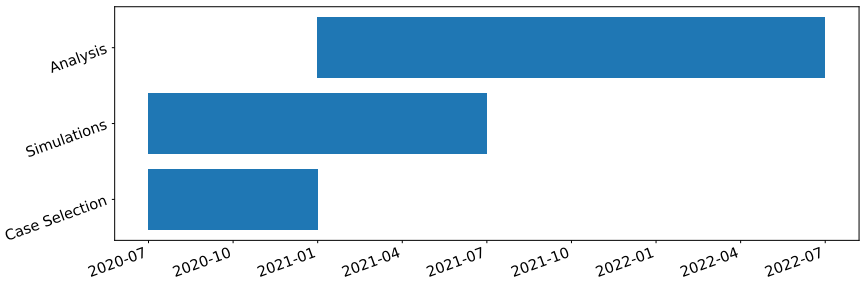

Figure 4: Timeline of proposed major research tasks

As such, I anticipate running experimental simulations to continue well into 2021, even as analysis of already-simulated cases is underway. Simulations should be completely wrapped-up by summer 2021, with the next year dedicated to analysis of the data. However, there is a strong possibility of new questions and new experiments developing during that time, along with technical difficulties in properly modeling cases, so the simulations timeline may be extended. A visualization of this timeline is shown in Figure 4.

7 Summary and Broader Impacts

This document outlines proposed research on Arctic mixed-phase stratocumulus clouds. Specifically, the questions posed in Section 1 relate to the tenuous cloud regime observed in Mauritsen et al. (2011) and simulated in Birch et al. (2012); Stevens et al. (2018). Field sites will be used to identify potential cases of cloud dissipation caused by a lack of available CCN. Large Eddy Simulations will be performed on identified tenuous cloud dissipation cases, and results analyzed to identify the microphysical processes at play. Mixed-phase clouds are inherently complex and not well understood, and the work proposed will serve to further our scientific understanding of the physics governing the formation, persistence, and dissipation of these unique clouds. The proposed research will also improve upon work already done on this subject by Tong (2019), namely by providing a stable control simulation, simulating a wider range of cases, and adjusting the aerosol treatment in the boundary layer.

The broader goal of the research is to further the scientific understanding of the processes that control Arctic boundary layer clouds and improve their representation in numerical models. Clouds are incredibly important to Arctic surface warming under climate change, and understanding the Arctic's response to warming is crucial to quantifying sea level rise and other direct climate impacts. The Arctic has proven to be a difficult location for global climate models to predict accurately, and any improvement on the understanding of Arctic processes has the potential to directly affect their representation climate models.

8 Bibliography

Bergeron, T. (1935). On the physics of clouds and precipitation. *Proc. 5th Assembly U.G.G.I., Lisbon, Portugal, 1935*, pages 156–180.

Birch, C. E., Brooks, I. M., Tjernström, M., Shupe, M. D., Mauritsen, T., Sedlar, J., Lock, A. P., Earnshaw, P., Persson, P. O. G., Milton, S. F., and Leck, C. (2012). Modelling atmospheric structure, cloud and their response to CCN in the central Arctic: ASCOS case studies. *Atmospheric Chemistry and Physics*, 12(7):3419–3435. Publisher: Copernicus GmbH.

Brooks, I. M., Tjernström, M., Persson, P. O. G., Shupe, M. D., Atkinson, R. A., Canut, G., Birch, C. E., Mauritsen, T., Sedlar, J., and Brooks, B. J. (2017). The Turbulent Structure of the Arctic Summer Boundary Layer During The Arctic Summer Cloud-Ocean Study. *Journal of Geophysical Research: Atmospheres*, 122(18):9685–9704.

Cheng, M. D., Hopke, P. K., Barrie, L., Rippe, A., Olson, M., and Landsberger, S. (1993). Qualitative determination of source regions of aerosol in Canadian high Arctic. *Environmental Science & Technology*, 27(10):2063–2071.

Cotton, W. R., Pielke Sr., R. A., Walko, R. L., Liston, G. E., Tremback, C. J., Jiang, H., McAnelly, R. L., Harrington, J. Y., Nicholls, M. E., Carrio, G. G., and McFadden, J. P. (2003). RAMS 2001: Current status and future directions. *Meteorology and Atmospheric Physics*, 82(1):5–29.

Cotton, W. R., Stevens, B., Feingold, G., and Walko, R. L. (1992). Large eddy simulation of marine stratocumulus cloud with explicit microphysics. In *proceedings of a workshop on parameterization of the cloud topped boundary layer. ECMWF, Reading RG29AX, UK*, volume 236.

DeMott, P. J., Prenni, A. J., Liu, X., Kreidenweis, S. M., Petters, M. D., Twohy, C. H., Richardson, M. S., Eidhammer, T., and Rogers, D. C. (2010). Predicting global atmospheric ice nuclei distributions and their impacts on climate. *Proceedings of the National Academy of Sciences*, 107(25):11217–11222. Publisher: National Academy of Sciences Section: Physical Sciences.

Egerer, U., Ehrlich, A., Gottschalk, M., Neggers, R. A. J., Siebert, H., and Wendisch, M. (2020). Case study of a humidity layer above Arctic stratocumulus using balloon-borne turbulence and radiation measurements and large eddy simulations. *Atmospheric Chemistry and Physics Discussions*, pages 1–27. Publisher: Copernicus GmbH.

Findeisen, W. (1938). Kolloid-meteorologische Vorgänge bei Neiderschlags-bildung. *Meteor. Z*, 55:121–133.

Garrett, T. J., Radke, L. F., and Hobbs, P. V. (2002). Aerosol Effects on Cloud Emissivity and Surface Longwave Heating in the Arctic. *Journal of the Atmospheric Sciences*, 59(3):769–778. Publisher: American Meteorological Society.

Garrett, T. J. and Zhao, C. (2006). Increased Arctic cloud longwave emissivity associated with pollution from mid-latitudes. *Nature*, 440(7085):787–789. ISBN: 1476-4687.

Gunsch, M. J., Liu, J., Moffett, C. E., Sheesley, R. J., Wang, N., Zhang, Q., Watson, T. B., and Pratt, K. A. (2019). Diesel Soot and Amine-Containing Organic Sulfate Aerosols in an Arctic Oil Field. *Environmental Science & Technology*, page acs.est.9b04825.

Harrington, J. Y. (1997). *The effects of radiative and microphysical processes on simulated warm and transition season Arctic stratus*. PhD thesis, Colorado State University.

Holland, M. M. and Bitz, C. M. (2003). Polar amplification of climate change in coupled models. *Climate Dynamics*, 21(3):221–232.

Igel, A. L., Ekman, A. M. L., Leck, C., Tjernström, M., Savre, J., and Sedlar, J. (2017). The free troposphere as a potential source of arctic boundary layer aerosol particles. *Geophysical Research Letters*, 44(13):7053–7060.

Intrieri, J. M., Fairall, C. W., Shupe, M. D., Persson, P. O. G., Andreas, E. L., Guest, P. S., and Moritz, R. E. (2002). An annual cycle of Arctic surface cloud forcing at SHEBA. *Journal of Geophysical Research: Oceans*, 107(C10):SHE 13–1–SHE 13–14.

Jiang, H. and Feingold, G. (2006). Effect of aerosol on warm convective clouds: Aerosol-cloud-surface flux feedbacks in a new coupled large eddy model. *Journal of Geophysical Research: Atmospheres*, 111(D1).

Jiang, H., Feingold, G., Cotton, W. R., and Duynkerke, P. G. (2001). Large-eddy simulations of entrainment of cloud condensation nuclei into the Arctic boundary layer: May 18, 1998, FIRE/SHEBA case study. *Journal of Geophysical Research: Atmospheres*, 106(D14):15113–15122. _eprint: https://agupubs.onlinelibrary.wiley.com/doi/pdf/10.1029/2000JD900303.

Klein, S. A., McCoy, R. B., Morrison, H., Ackerman, A. S., Avramov, A., de Boer, G., Chen, M., Cole, J. N., del Genio, A. D., Falk, M., Foster, M. J., Fridlind, A., Golaz, J. C., Hashino, T., Harrington, J. Y., Hoose, C., Khairoutdinov, M. F., Larson, V. E., Liu, X., Luo, Y., McFarquhar, G. M., Menon, S., Neggers, R. A., Park, S., Poellot, M. R., Schmidt, J. M., Sednev, I., Shipway, B. J., Shupe, M. D., Spangenberg, D. A., Sud, Y. C., Turner, D. D., Veron, D. E., von Salzen, K., Walker, G. K., Wang, Z., Wolf, A. B., Xie, S., Xu, K. M., Yang, F., and Zhang, G. (2009). Intercomparison of model simulations of mixed-phase clouds observed during the ARM Mixed-Phase Arctic Cloud Experiment. I: Single-layer cloud. *Quarterly Journal of the Royal Meteorological Society*, 135(641):979–1002. ISBN: 1477-870X.

Korolev, A. (2007). Limitations of the Wegener–Bergeron–Findeisen Mechanism in the Evolution of Mixed-Phase Clouds. *Journal of the Atmospheric Sciences*, 64(9):3372–3375. Publisher: American Meteorological Society.

Kupiszewski, P., Leck, C., Tjernström, M., Sjogren, S., Sedlar, J., Graus, M., Müller, M., Brooks, B., Swietlicki, E., Norris, S., and Hansel, A. (2013). Vertical profiling of aerosol

particles and trace gases over the central Arctic Ocean during summer. *Atmospheric Chemistry and Physics*, 13(24):12405–12431. Publisher: Copernicus GmbH.

Mauritsen, T., Sedlar, J., Tjernstrom, M., Leck, C., Martin, M., Shupe, M., Sjögren, S., Sierau, B., Persson, P. O. G., and Brooks, I. M. (2011). An Arctic CCN-limited cloud-aerosol regime. *Atmospheric Chemistry and Physics*, 11(1):165–173. Number: 1 Publisher: European Geosciences Union.

Meyers, M. P., Walko, R. L., Harrington, J. Y., and Cotton, W. R. (1997). New rams cloud microphysics parameterization. part ii: The two-moment scheme. *Atmospheric Research*, 45(1):3–39.

Morrison, H., De Boer, G., Feingold, G., Harrington, J., Shupe, M. D., and Sulia, K. (2012). Resilience of persistent Arctic mixed-phase clouds. *Nature Geoscience*, 5(1):11–17. Publisher: Nature Publishing Group.

Morrison, H., Zuidema, P., Ackerman, A. S., Avramov, A., De Boer, G., Fan, J., Fridlind, A. M., Hashino, T., Harrington, J. Y., Luo, Y., Ovchinnikov, M., and Shipway, B. (2011). Intercomparison of cloud model simulations of Arctic mixed-phase boundary layer clouds observed during SHEBA/FIRE-ACE. *Journal of Advances in Modeling Earth Systems*, 3(2). Publisher: Blackwell Publishing Ltd.

Naakka, T., Nygård, T., and Vihma, T. (2018). Arctic Humidity Inversions: Climatology and Processes. *Journal of Climate*, 31(10):3765–3787. Publisher: American Meteorological Society.

Prenni, A. J., Harrington, J. Y., Tjernström, M., DeMott, P. J., Avramov, A., Long, C. N., Kreidenweis, S. M., Olsson, P. Q., and Verlinde, J. (2007). Can Ice-Nucleating Aerosols Affect Arctic Seasonal Climate? *Bulletin of the American Meteorological Society*, 88(4):541–550. Publisher: American Meteorological Society.

Rahn, K. A., Borys, R. D., and Shaw, G. E. (1977). The Asian source of Arctic haze bands. *Nature*, 268(5622):713–715.

Saleeby, S. M. and Cotton, W. R. (2004). A Large-Droplet Mode and Prognostic Number Concentration of Cloud Droplets in the Colorado State University Regional Atmospheric Modeling System (RAMS). Part I: Module Descriptions and Supercell Test Simulations. *Journal of Applied Meteorology*, 43(1):182–195. Publisher: American Meteorological Society.

Saleeby, S. M. and van den Heever, S. C. (2013). Developments in the CSU-RAMS Aerosol Model: Emissions, Nucleation, Regeneration, Deposition, and Radiation. *Journal of Applied Meteorology and Climatology*, 52(12):2601–2622. Publisher: American Meteorological Society.

Sedlar, J., Shupe, M. D., and Tjernström, M. (2012). On the Relationship between Thermodynamic Structure and Cloud Top, and Its Climate Significance in the Arctic. *Journal of Climate*, 25(7):2374–2393.

Sedlar, J. and Tjernström, M. (2009). Stratiform Cloud—Inversion Characterization During the Arctic Melt Season. *Boundary-Layer Meteorology*, 132(3):455–474.

Sedlar, J., Tjernström, M., Mauritsen, T., Shupe, M. D., Brooks, I. M., Persson, P. O. G., Birch, C. E., Leck, C., Sirevaag, A., and Nicolaus, M. (2011). A transitioning Arctic surface energy budget: The impacts of solar zenith angle, surface albedo and cloud radiative forcing. *Climate Dynamics*, 37(7-8):1643–1660.

Shupe, M. D. (2011). Clouds at Arctic Atmospheric Observatories. Part II: Thermodynamic Phase Characteristics. *Journal of Applied Meteorology and Climatology*, 50(3):645–661. Publisher: American Meteorological Society.

Shupe, M. D. and Intrieri, J. M. (2004). Cloud Radiative Forcing of the Arctic Surface: The Influence of Cloud Properties, Surface Albedo, and Solar Zenith Angle. *Journal of Climate*, 17(3):616–628. Publisher: American Meteorological Society.

Shupe, M. D., Matrosov, S. Y., and Uttal, T. (2006). Arctic Mixed-Phase Cloud Properties Derived from Surface-Based Sensors at SHEBA. *Journal of the Atmospheric Sciences*, 63(2):697–711. Publisher: American Meteorological Society.

Solomon, A., Shupe, M. D., Persson, P. O. G., and Morrison, H. (2011). Moisture and dynamical interactions maintaining decoupled Arctic mixed-phase stratocumulus in the presence of a humidity inversion. *Atmospheric Chemistry and Physics*, 11(19):10127–10148. Publisher: Copernicus GmbH.

Sotiropoulou, G., Bossioli, E., and Tombrou, M. (2019). Modeling Extreme Warm-Air Advection in the Arctic: The Role of Microphysical Treatment of Cloud Droplet Concentration. *Journal of Geophysical Research: Atmospheres*, 124(6):3492–3519. _eprint: https://agupubs.onlinelibrary.wiley.com/doi/pdf/10.1029/2018JD029252.

Stevens, R. G., Loewe, K., Dearden, C., Dimitrelos, A., Possner, A., Eirund, G. K., Raatikainen, T., Hill, A. A., Shipway, B. J., Wilkinson, J., Romakkaniemi, S., Tonttila, J., Laaksonen, A., Korhonen, H., Connolly, P., Lohmann, U., Hoose, C., Ekman, A. M., Carslaw, K. S., and Field, P. R. (2018). A model intercomparison of CCN-limited tenuous clouds in the high Arctic. *Atmospheric Chemistry and Physics*, 18(15):11041–11071. ISBN: 1680-7316.

Tjernström, M., Leck, C., Birch, C. E., Bottenheim, J. W., Brooks, B. J., Brooks, I. M., Bäcklin, L., Chang, R. Y., De Leeuw, G., Di Liberto, L., De La Rosa, S., Granath, E., Graus, M., Hansel, A., Heintzenberg, J., Held, A., Hind, A., Johnston, P., Knulst, J., Martin, M., Matrai, P. A., Mauritsen, T., Müller, M., Norris, S. J., Orellana, M. V., Orsini, D. A., Paatero, J., Persson, P. O., Gao, Q., Rauschenberg, C., Ristovski, Z., Sedlar, J., Shupe, M. D., Sierau, B., Sirevaag, A., Sjogren, S., Stetzer, O., Swietlicki, E., Szczodrak, M., Vaattovaara, P., Wahlberg, N., Westberg, M., and Wheeler, C. R. (2014). The Arctic Summer Cloud Ocean Study (ASCOS): Overview and experimental design. *Atmospheric Chemistry and Physics*, 14(6):2823–2869.

Tong, S. (2019). Impacts of Aerosol Concentration on the Dissipation of Arctic Mixed-Phase Clouds. Master's thesis, University of California, Davis. ProQuest Dissertations & Theses.

Turner, D. D., Clough, S. A., Liljegren, J. C., Clothiaux, E. E., Cady-Pereira, K. E., and Gaustad, K. L. (2007). Retrieving Liquid Wat0er Path and Precipitable Water Vapor From the Atmospheric Radiation Measurement (ARM) Microwave Radiometers. *IEEE Transactions on Geoscience and Remote Sensing*, 45(11):3680–3690. Conference Name: IEEE Transactions on Geoscience and Remote Sensing.

Twomey, S. (1977). The Influence of Pollution on the Shortwave Albedo of Clouds. *Journal of the Atmospheric Sciences*, 34(7):1149–1152. Publisher: American Meteorological Society.

Walko, R., Cotton, W., Meyers, M., and Harrington, J. (1995). New RAMS cloud microphysics parameterization part I: the single-moment scheme. *Atmospheric Research*, 38(1-4):29–62.

Wegener, A. (1911). *Thermodynamik der atmosphäre*. J. A. Barth. Google-Books-ID: kWtUAAAAMAAJ.